Biochemical and Biophysical Research Communications 448 (2014) 461–466

Contents lists available at ScienceDirect

Biochemical and Biophysical Research Communications

journal homepage: www.elsevier.com/locate/ybbrc

Cancer cells recovering from damage exhibit mitochondrial restructuring and increased aerobic glycolysis

Shin Akakura [a], Elena Ostrakhovitch [a], Reiko Sanokawa-Akakura [a], Siamak Tabibzadeh [a,b,*]

[a] Frontiers in Bioscience Research Institute in Aging and Cancer, University of California, Irvine, CA, USA
[b] Dept of Oncologic Radiology, University of California, Irvine, CA, USA

ARTICLE INFO

Article history:
Received 22 April 2014
Available online 4 May 2014

Keywords:
Damage
Tolerance
Proliferation
Mitochondria

ABSTRACT

Instead of relying on mitochondrial oxidative phosphorylation, most cancer cells rely heavily on aerobic glycolysis, a phenomenon termed as "the Warburg effect". We considered that this effect is a direct consequence of damage which persists in cancer cells that recover from damage. To this end, we studied glycolysis and rate of cell proliferation in cancer cells that recovered from severe damage. We show that *in vitro* Damage-Recovered (DR) cells exhibit mitochondrial structural remodeling, display Warburg effect, and show increased *in vitro* and *in vivo* proliferation and tolerance to damage. To test whether cancer cells derived from tumor microenvironment can show similar properties, we isolated Damage-Recovered (T^{DR}) cells from tumors. We demonstrate that T^{DR} cells also show increased aerobic glycolysis and a high proliferation rate. These findings show that Warburg effect and its consequences are induced in cancer cells that survive severe damage.

1. Introduction

Most cancer cells utilize aerobic glycolysis for their energy needs (Warburg effect), despite the fact that this pathway is an inefficient way to generate adenosine 5′-triphosphate (ATP) when oxygen is abundant [1–3]. It is still not well understood as why such a less efficient metabolism is selected by proliferating cancer cells. One reasonable explanation would be that inefficient ATP production happens only when energy resources are scarce, such as in areas of the tumor where low blood flow leads to low nutrient, hypoxic and an acidotic conditions [4]. However, some cancer cells appear to rely on glycolytic metabolism even before they are exposed to such harsh conditions [5–8]. Some consider that the adoption of aerobic glycolysis by cancer cells is driven by tumor hypoxia [9] while others consider that aerobic glycolysis might be multi-factorial and driven by oncogenes, tumor suppressors, mtDNA mutations and other factors [9–11].

In this study, we aimed to address whether the Warburg effect might be a consequence of damage which occurs in hypovascularized regions of tumors that create hypoxia, glucopenia and acidosis. We demonstrate here that cancer cells that recover from such damages exhibit mitochondrial structural changes including development of a primordial type as evidenced by ballooning and remodeling of cristae. These changes are associated with decreased copy number of mtDNA, increased expression of glycolytic enzymes, activation of glycolytic system of energy production, increased ATP synthesis, increased tolerance to damage as well as rapid *in vitro* and *in vivo* proliferation. We also show that cells that recover from damage endured *in vivo* are also highly glycolytic and exhibit a high rate of cell proliferation. These findings suggest a role for damage-recovery in the adoption of "Warburg effect" by the tumor cells. Furthermore, these data indicate that cancer cells that emerge after recovery from damage, display new metabolic characteristics consistent with a higher degree of malignant behavior as evidenced by damage tolerance and increased rate of cell proliferation.

2. Materials and methods

2.1. Reagents and cell culture

Chemicals were from Sigma-Aldrich (St. Louis, MO) or Fisher Scientific (Pittsburgh, PA). Trypan Blue was purchased from

Abbreviations: Pc, parental control; DR, Damage-Recovered; T^{V}, Viable tumor derived cells; T^{DR}, Damage-Recovered tumor derived cells; ECAR, extracellular acidification rates; ATP, adenosine 5′-triphosphate; AUC, area under the curve; BrdU, 5-bromo-2′-deoxyuridine; *CYT B* and *C*, *CYTOCHROME B* and *C*; 2DG, 2-deoxyglucose; *ENTPD5*, ectonucleoside triphosphate diphosphohydrolase 5; FCCP, carbonyl cyanide-4-(trifluoromethoxy) phenylhydrazone; *HK1*, *HEXOKINASE 1*; *LDH A*, lactate dehydrogenase A; *mtTFA*, mitochondrial transcription factor A.

* Corresponding author. Address: 16471 Scientific Way, Irvine, CA 92618, USA.
E-mail address: fbs@bioscience.org (S. Tabibzadeh).

http://dx.doi.org/10.1016/j.bbrc.2014.04.138
0006-291X/

Sigma-Aldrich and staining was performed as described by the manufacturer. Collagenase-P was purchased from Roche Applied Science (Indianapolis, IN). RNAlater™ RNA Stabilization Reagent and RNeasy Mini Kit for total RNA isolation were purchased from Qiagen Inc. (Valencia, CA). The antibodies were from Millipore (Billerica, MA), Invitrogen (Carlsbad, CA) and Jackson ImmunoResearch Laboratories (Baltimore, PA). CT26 mouse colon carcinoma cell line (CRL-2639) was obtained from ATCC (Manassas, VA), and maintained in RPMI 1640 with 2 mM glutamine, 10 mM HEPES, 1 mM sodium pyruvate, 25 mM glucose, 1.5 g/L sodium bicarbonate and 10% fetal bovine serum in 37 °C incubator with 5% CO_2. Condition of damages were as follows; for induction of heat induced damage (DR^{He}), cells were incubated at 45 °C for 45 min, for induction of hypoxic damage (DR^{H}), cells were incubated in 0.3% O_2 at 37 °C, and for damage induced by glucose deprivation (DR^{G-}), cells were cultured in a medium with no glucose in 5% CO_2 at 37 °C. For induction of damage by acidosis (DR^{A}), cells were cultured in RPMI-based medium, pH was adjusted to 6.0 and cells were incubated in 5% CO_2 at 37 °C. Cultures were subjected to hypoxia, glucose deprivation, and acidosis for 3–5 days until majority of cells were lost due to cell death.

2.2. Animal experiments and isolation of cancer cells derived from in vivo grown tumors

Animal care and all procedures carried out on animals were approved by the Institutional Animal Care Committees at University of California, Irvine. Each athymic nude (NOD/SCID) mouse received 10^5 cancer cells in a total volume of 200 µl subcutaneously in four locations in the mid-abdominal and lower flank areas after anesthesia. Tumors were removed and weighed. Tumors were minced into <1 mm blocks, and incubated with 250 µg/ml Collagenase-P at 37 °C for 20 min. Suspension of single tumor cells were >95% viable (T^{V}) as determined by Trypan blue staining. Sedimented small fragments that settled to the bottom of the tubes were comprised of apoptotic regions with large areas of Trypan blue positive cells. These fragments were subjected to treatment with 0.25% trypsin at 37 °C for 10 min. Majority (>95%) of single cells in the cell suspension after incubation were Trypan blue positive. This cell suspension was cultured for 24 h to allow viable cells to bind to the culture substrate. The floating cells were subsequently transferred weekly to new culture vessels. Damaged cells that recovered (T^{DR}) and started to proliferate were collected after 2 weeks.

2.3. Immunostaining

Cells were fixed for 5 min in 2% buffered paraformaldehyde containing 0.02% NP40, and subjected to blocking for 10 min in 2% serum. For γH_2AX staining, cells were incubated with anti-γH2AX antibody conjugated with biotin (1–2 µg/ml; Millipore) followed by Peroxidase-Streptavidin (0.1 µg/ml; Jackson ImmunoResearch). The γH2AX staining was developed in 3,3′-diaminobenzidine (DAB)-H_2O_2 (DAKO; Carpinteria, CA) and viewed at the light microscopic level without counterstain. For BrdU staining, cells were incubated with anti-BrdU antibody conjugated with biotin (1–2 µg/ml; Invitrogen) followed by Tetra-methyl Rhodamine-Streptavidin (0.1 µg/ml; Jackson ImmunoResearch). The fluorescent images were

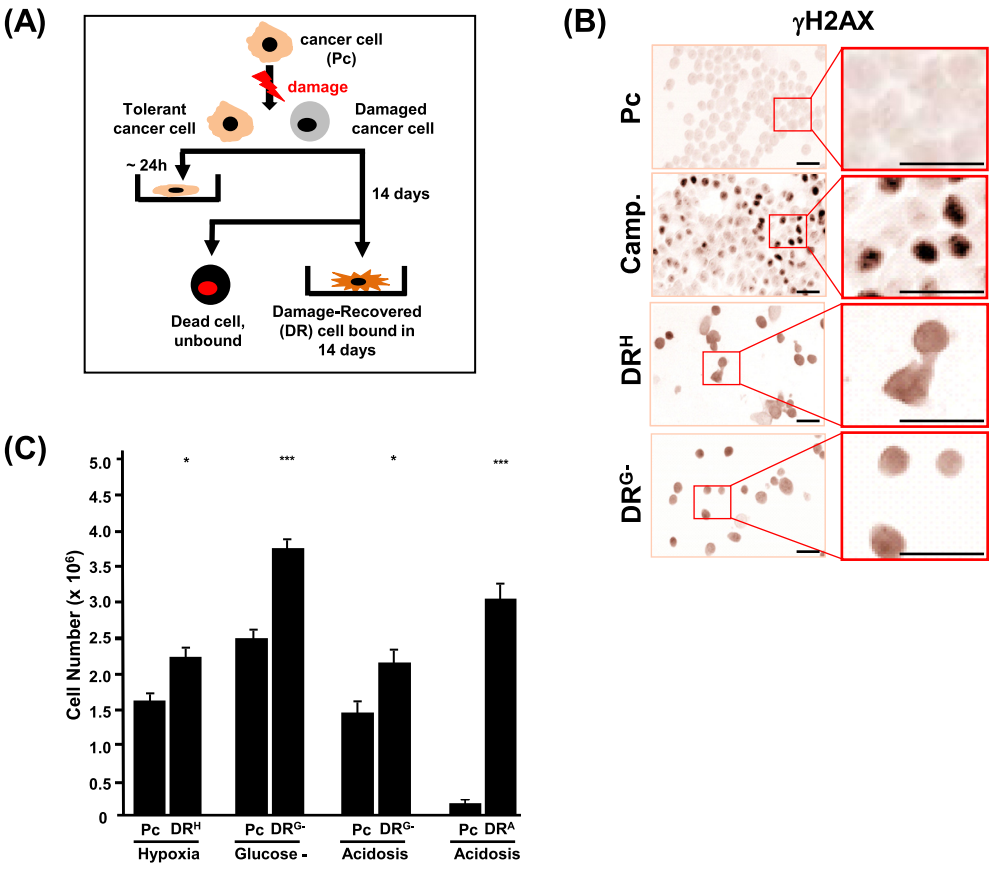

Fig. 1. Damage-Recovered (DR) cells show increased tolerance to damage. (A) Scheme for isolation of DR cells after damage by heat (DR^{He}), hypoxia (DR^{H}), glucose deprivation (DR^{G-}) and acidosis (DR^{A}). (B) Immunostaining of γH2AX in Pc, camptothecin-treated Pc, DR^{H} and DR^{G-} CT26 cells. Scale bars, 50 µM. (C) Number of DR cells remaining after being subjected to hypoxia, glucose deprivation and acidosis after 5 days. Culture dishes were seeded with 2.5×10^6 cells in triplicate and the number of viable cells was determined by Trypan blue staining. $^{*}p < 0.05$, $^{**}p < 0.005$, $^{***}p < 0.0005$.

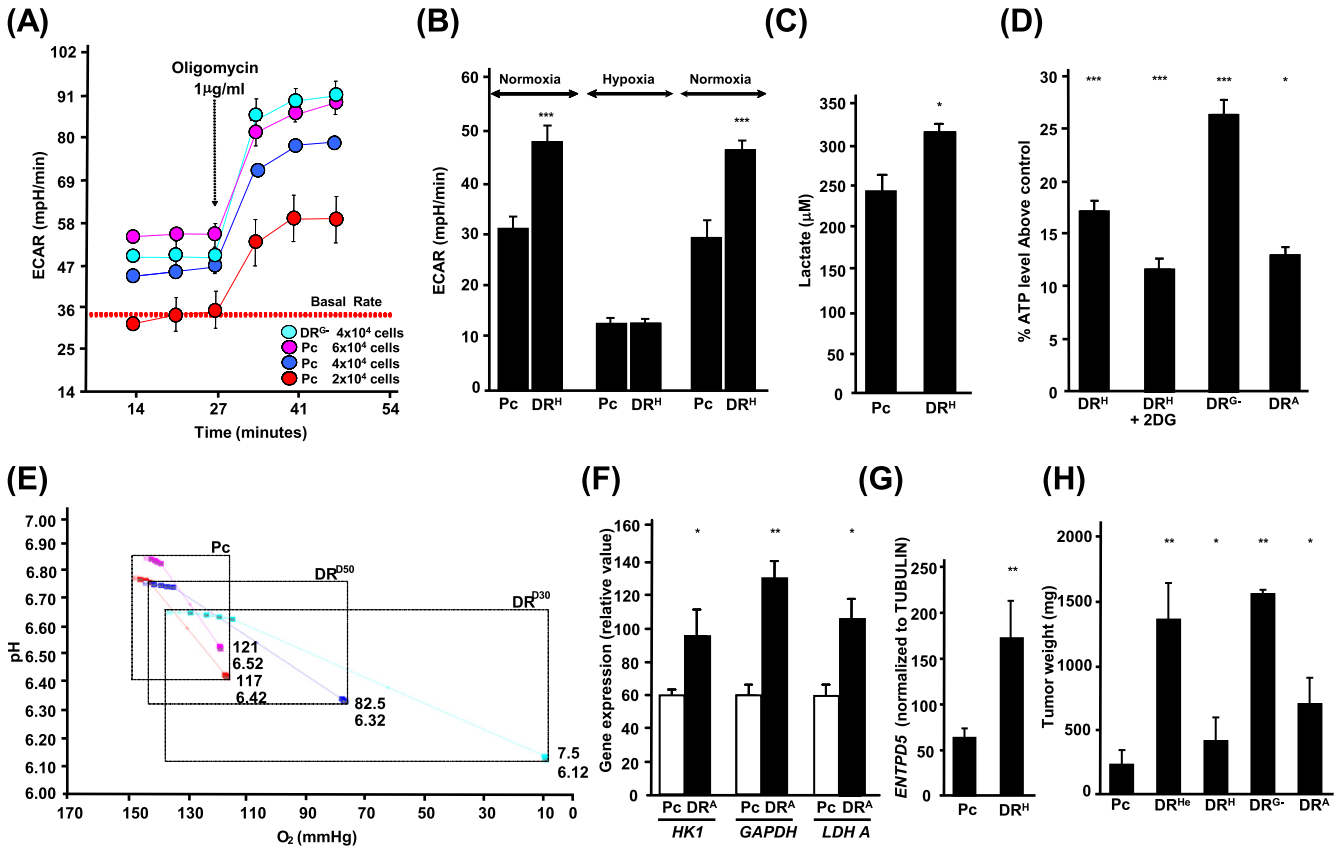

Fig. 2. DR cells exhibit an increased aerobic glycolysis. (A) ECAR of 2×10^4, 4×10^4, and 6×10^4 of Pc and 4×10^4 of DR^{G-} CT26 cells subjected to oligomycin after three basal measurements. The basal rate of ECAR of DR cells is higher than the ECAR of the same number of Pc cells. After treatment with oligomycin, the ECAR of DR cells exceeds the ECAR of the same number of Pc cells by 1.5-fold. B. ECAR in Pc and DR^H CT26 cells during normoxia and hypoxia. After three basal measurements, to induce hypoxia, ECAR was measured 15 times without mixing. Then, mixing was allowed to restore normoxia and then three more measurements of ECAR were made. C. Media of cultures of Pc and DR^H CT26 cells (1×10^6 cells) were collected after 3 days and lactate was measured by ELISA. Lactate levels were normalized by the number of cells in the culture. (D) ATP levels in DR^H CT26 cells in presence and absence of 2DG (20 μM, 48 h), and in DR^{G-} and DR^A CT26 cells. (E) Level of pH and pO_2 before and after induction of hypoxia in Pc, and DR^A CT26 cells on day 30 (D^{30}) and day 50 (D^{50}). The pH (top number) and pO_2 (bottom number) are shown in the left lower corner of rectangles. (F) Expression level of *HEXOKINASE* (*HK1*), *GAPDH* and *LDH A* assessed by real time PCR in Pc and DR^A CT26 cells. (G) Expression level of *ENTPD5* assessed by real time PCR in Pc and DR^H CT26 cells. (H) Weight of tumors that grew for 15 days subcutaneously *in vivo* in athymic nude mice after injection of 2×10^6 cells. Cells injected were Pc, DR^{He}, DR^H, DR^{G-} and DR^A CT26 cells. $^*p < 0.05$, $^{**}p < 0.005$, $^{***}p < 0.0005$.

visualized using fluorescent microscope (Olympus IX50; Center Valley, PA), and images were captured with MagnaFire-SP® software (OPTRONICS, Inc.; Goleta, CA), and the number of positive cells were counted in a minimum of 300 total cells.

2.4. XF (extracellular flux) bioenergetic analysis

XF24 Extracellular Flux Analyzer from Seahorse Bioscience (North Billerica, MA) was utilized for extracellular fluid bioenergetic analysis [12], and the assay was performed according to the manufacturer's instruction. Briefly, five control (4×10^4) and five experimental cell samples (4×10^4) were plated in each well of the XF 24 culture plate and cells were incubated overnight at 37 °C in presence of 5% CO_2. All cultures were examined in XFAssay media in the absence of CO_2. pH and pO_2 were measured by XF analyzer on the subsequent day. After two basal measurements with mixing, 15 repeated measurements were carried out without mixing to induce hypoxia. Unless stated otherwise, cells were cultured at 4×10^4 cells per well and treated with oligomycin (1 μg/ml), followed by 5 μM FCCP.

2.5. Lactate and ATP assays

Lactate was quantitated using the Lactate Assay kit (Biovision; Milpitas, CA). ATP levels in cells was assayed using the Bioluminescent ATP Somatic cell assay kit (FLASC, Sigma–Aldrich) and colorimetric ATP assay kit (Abcam; Cambridge, MA) according to manufacturer's instruction. Levels of ATP, NAD^+, NADH and thiols were normalized to the protein content.

2.6. Quantitative PCR

Gene expression was assessed by qPCR using QuantiTect SYBR Green PCR Kit and DNA Engine Opticon system (Bio-Rad; Hercules, CA) according to manufacturer's instruction. Reverse transcription was performed using ProtoScript first strand cDNA synthesis Kit (New England Biolabs; Ipswich, MA) or high capacity cDNA reverse transcription kit (Invitrogen). Quantitative evaluation was performed by using myImage Analysis software (Thermo Scientific; Waltham, MA). Mitochondrial DNA was isolated using GenElute™ Mammalian Genomic DNA Miniprep Kit (Sigma–Aldrich). qPCR was performed using QuantiTect SYBR Green PCR Kit and DNA Engine Opticon system. For normalization of data, *β-ACTIN* or *TUBULIN* was amplified with specific primers.

2.7. Ultrastructural study

Cells were fixed in 2.5% glutaraldehyde, post-fixed in 1% osmium tetroxide, dehydrated in ascending series of alcohol and embedded in Epon. Thin sections (~80 nm thickness) were viewed

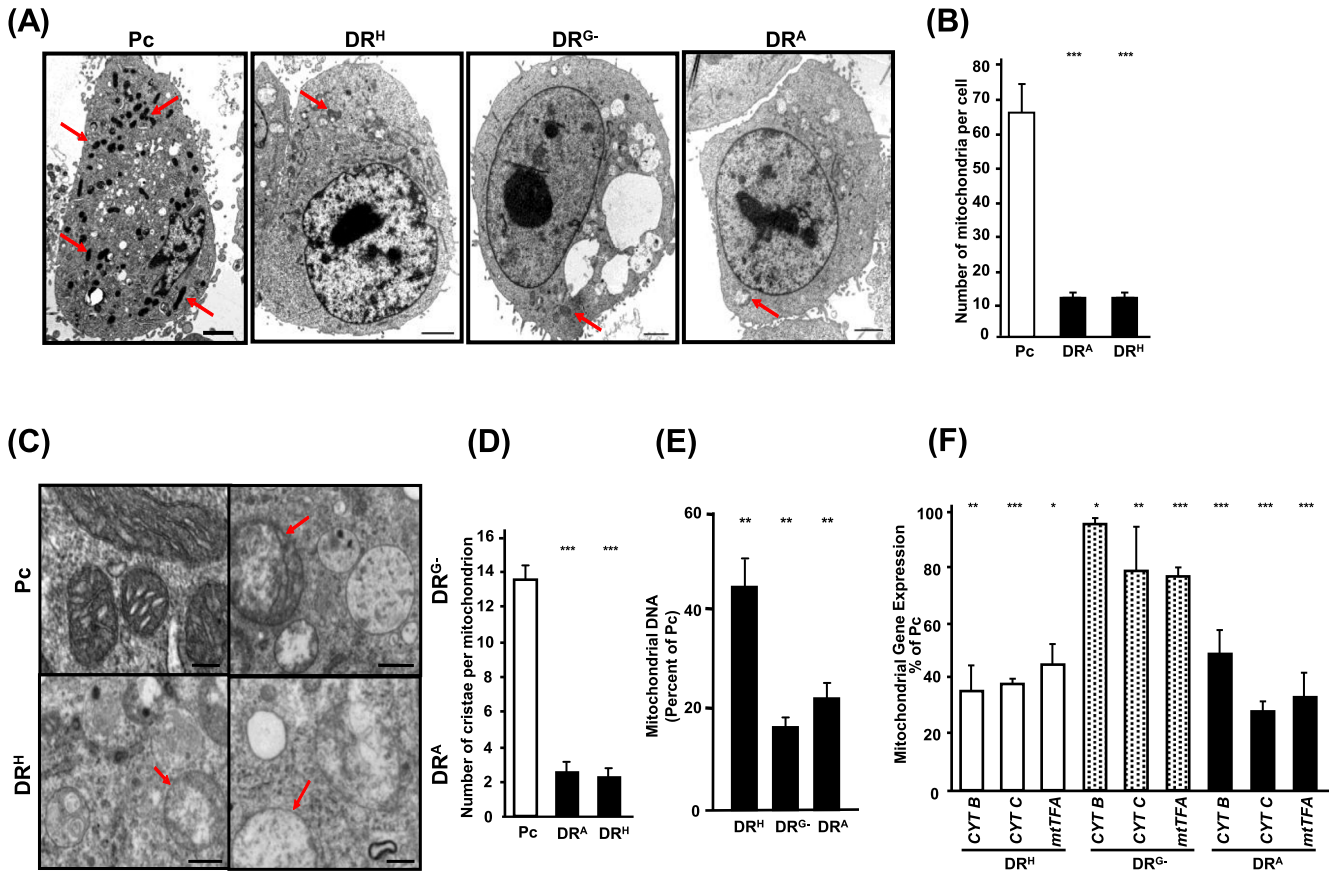

Fig. 3. Changes in mitochondrial morphology, number, and gene expression in cancer cells recovered from damage. (A) Transmission electron micrographs of Pc, DR^H, DR^{G-}, and DR^A CT26 cells. Arrows point to the mitochondria. Scale bars, 2 μM. (B) Number of mitochondria per cell in Pc, DR^A and DR^H CT26 cells. (C) TEM of Pc, DR^H, DR^{G-}, and DR^A CT26 cells. Arrows point to the mitochondria. Scale bars, 500 nm. (D) Number of cristae per mitochondrion in Pc, DR^A and DR^H CT26 cells. (E) Quantitation of mitochondrial DNA by real time PCR amplification of a 227 base pairs fragment of mouse mitochondrial *CYTOCHROME B* DNA in CT26 Pc versus DR^H, DR^{G-} and DR^A CT26 cells. Data are normalized to the expression level of *β-ACTIN*. (F) The expression level of *CYTOCHROME B* (*CYT B*), *CYTOCHROME C* (*CYT C*) and *MITOCHONDRIAL TRANSCRIPTION FACTOR A* (*mtTFA*) in DR^H, DR^{G-} and DR^A CT26 cells was quantitated by real time PCR and expressed as percent of that found in Pc CT26 cells. $^*p < 0.05$, $^{**}p < 0.005$, $^{***}p < 0.0005$.

at 80 kV with FEI Tecnai12 BioTwinG2 transmission electron microscope (Hillsboro, OR). Digital images were acquired with an AMT XR-60 CCD Digital Camera System (Woburn, MA). Number of mitochondria was determined in a minimum of 20 cells and their cristae were counted in a minimum of 250 mitochondria in thin sections.

2.8. Statistics

All assays were done in 3–6 replicates in at least three independent experiments. Data are shown as mean ± SEM. *p* values were determined by comparing the data from experimental versus control cells from at least three independent experiments or six replicates of the same experiment. Means and *p* values for experimental data were analyzed by subjecting the data to the two tailed t-test. *p* values less than 0.05 were considered significant. *p* Values are shown as <0.05 (*), <0.005 (**) or <0.0005 (***). For XF data analysis, mean and *p* values were determined by comparing area under the curve (AUC).

3. Results

3.1. Cancer cells following damage recovery exhibit increased tolerance to damage

CT26 murine colon carcinoma cells were exposed to hypoxia (^{H}), glucose deprivation ($^{G-}$), acidosis (^{Ac}) and heat (^{He}). Within 48–72 h, less than 10% of viable cells remained attached to the culture flask while majority (>90%) of cells detached from culture surface due to severe damage. To remove viable cells, we cultured detached floating cells in new culture vessels for 24 h (Fig. 1A). To isolate damaged cells that failed to bind to culture vessels within 24 h but had the potential to recover from damage, we transferred floating cells to new culture vessels weekly. Damaged cells that recovered (DR), bound to the culture substrate after two weeks and started to proliferate were collected.

While parental control (Pc) cells did not show nuclear γH_2AX staining, there was nuclear staining for H_2AX in DR cells suggesting presence of residual damage. This staining was less than that induced by treatment of cells with DNA damaging agent, Camptothecin (Fig. 1B). Next, we assessed the tolerance of DR cells to damage. As compared to Pc cells, DR cells exhibited resistance to the initial damaging condition (Fig. 1C). Intriguingly, DR^{G-} cells cultured under acidotic conditions showed cross tolerance to acidosis (Fig. 1C).

3.2. DR cells exhibit increased aerobic glycolysis

We examined the rate of glycolysis in DR cells. DR cells had an elevated extracellular acidification rate (ECAR) and released excess lactate (Fig. 2A–C). Aerobic glycolysis was apparent under normoxia and was relinquished under hypoxic condition (Fig. 2B). DR cells also exhibited an increased ATP production (Fig. 2D). The observed increase in ATP was independent of the type of dam-

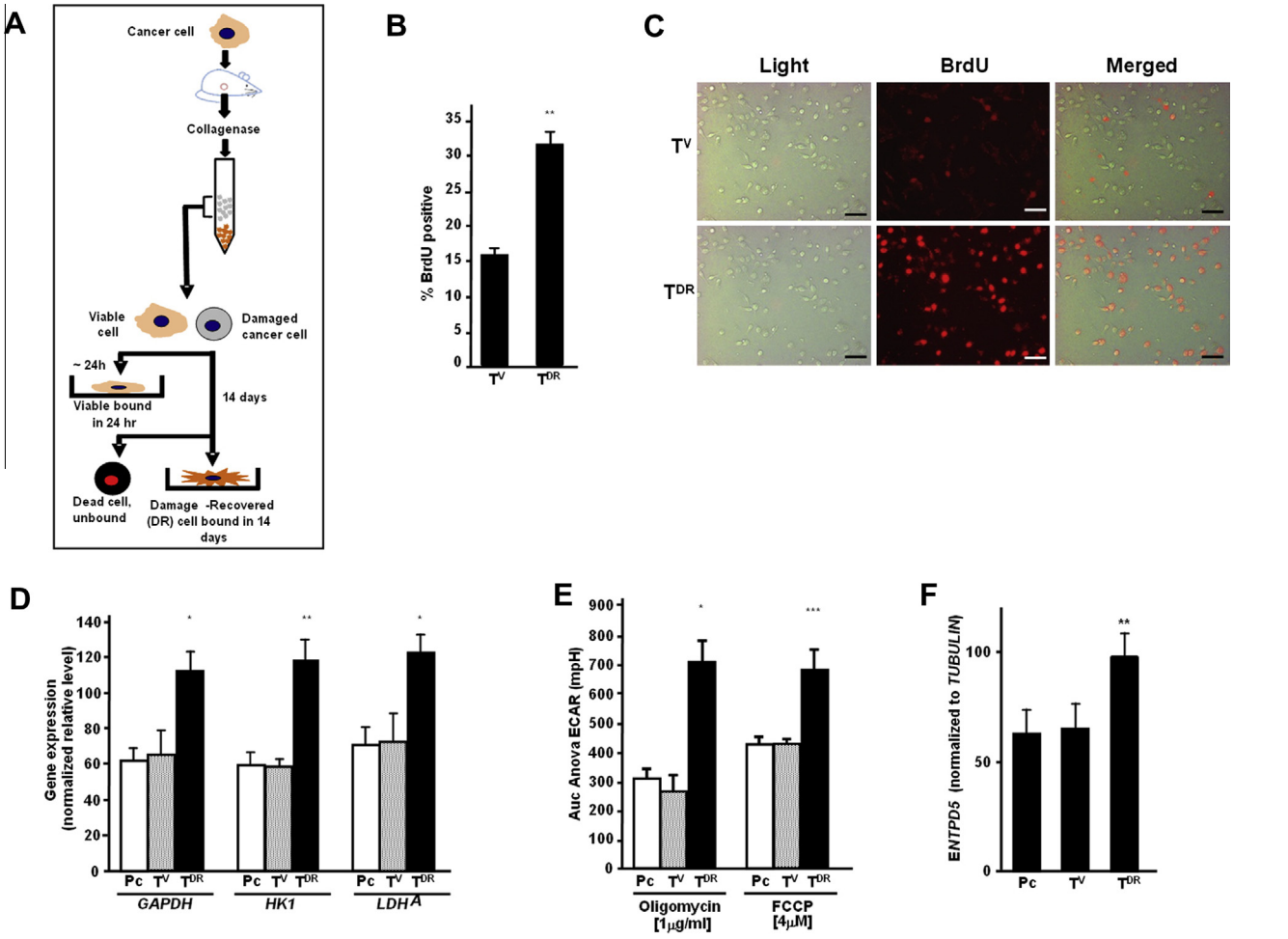

Fig. 4. Increased aerobic glycolysis in Damage-Recovered cancer cells isolated from *in vivo* generated tumors. (A) Scheme for isolation of T^V and T^{DR} CT26 cells used in this study. (B) Percentage of $BrdU^+$ cells in cultures of T^V and T^{DR} CT26 cells. (C) BrdU stained cells in T^V and T^{DR} CT26 cells. Scale bars, 50 μM. (D) Gene expression of *GAPDH*, *HK1*, and *LDH* A assessed by real time PCR in Pc, T^V and T^{DR} CT26 cells. Data are normalized to the expression level of *TUBULIN*. (E) AUC ANOVA of ECAR after treatment with oligomycin and FCCP in Pc, T^V and T^{DR} CT26 cells. (F) The expression level of *ENTPD5* assessed by real time PCR in Pc, T^V and T^{DR} CT26 cells. $^*p < 0.05$, $^{**}p < 0.005$, $^{***}p < 0.0005$.

age. Because of a heavy reliance on glycolysis, DR cells were more sensitive than Pc cells to the inhibition of aerobic glycolysis by 2-deoxyglucose (2DG) that caused a significant decrease in production of ATP in DR cells (Fig. 2D). Compared to Pc cells, DR cells exhibited rapid metabolism, which decreased the oxygen tension and pH in their microenvironment (Fig. 2E). The expression of genes that drive glycolysis including *HEXOKINASE 1* (*HK1*), *GAPDH*, *ENTPD5* and *LDH A* and lactate production were increased in DR cells (Fig. 2F). DR cells also showed increased *ENTPD5* which is shown to drive Warburg effect [13]. DR cells inoculated to immunodeficient mice formed tumors that grew significantly larger than those produced by Pc cells within the same time frame (Fig. 2H). These data indicate that DR cells have a higher *in vivo* growth rate and that they can sustain the tumor progeny and contribute to generation of tumors.

3.3. DR cells show bioenergetic remodeling of mitochondria including change in their morphology, number, DNA content and gene expression

In order to examine whether mitochondrial organization has been changed in DR cells, we assessed DR cells at the ultrastructural level. We found that the number of mitochondria was decreased in all DR cells (Fig. 3A and B). In contrast to mature tubular and cristae-rich somatic mitochondria in Pc cells, DR cells had a ballooned and a primordial appearance (Fig. 3A and C). Regardless of the cause of damage, DR cells exhibited sparse round cristae-poor mitochondria (Fig. 3C and D). A corresponding decrease in the level of mitochondrial DNA was also observed (Fig. 3E). These changes were associated with a coordinate decrease in *CYTOCHROME B*, *C* and *mtTFA* (Fig. 3F). These data indicate that DR cells exhibit mitochondrial structural remodeling.

3.4. Damage recovered cancer cells isolated from in vivo tumors demonstrate increased aerobic glycolysis

In order to identify whether cells similar to the *in vitro* generated DR cells are generated in tumors, cancer cells were inoculated into immunodeficient mice. Tumors that grew subcutaneously were removed, and were subjected to collagenase treatment. To remove viable tumor cells, suspensions of single tumor cells were added to new culture vessels and cells that bound to the dish were collected after 24 h (Fig. 4A). To isolate damaged cells that failed to bind to culture vessels within 24 h but had the potential to recover from damage, we transferred floating cells to new culture vessels weekly. Damaged cells that recovered (T^{DR}), bound to the culture substrate after two weeks and started to proliferate were collected. As compared to the T^v, T^{DR} cells had a higher rate of cell proliferation (Fig. 4B and C). T^{DR} cells also displayed a glycolytic phenotype characterized by up-regulation of *HEXOKINASE* (*HK1*), *GAPDH*, and *LDH* (Fig. 4D and E). As compared to the Pc and T^v cells, T^{DR} cells showed enhanced glycolysis as evidenced by increased ECAR

(Fig. 4E). Similar to DR cells, T^{DR} cells also showed increased expression of *ENTPD5* (Fig. 4E).

4. Discussion

It is well known that tumor cells can recover from various types of damage. The term Potentially Lethal Damage Recovery (PLDR) was first coined by Phillips and Tolmach. These authors showed that the response of cells to irradiation can be modified by various post-treatment conditions that interfere with processes that normally result in either repair or expression of damage [14]. For example, pH and glucose level play a crucial role in recovery of cancer cells from damage [15–17]. We demonstrate, here, that cancer cells can recover from a variety of damages such as hypoxia, acidosis and glucose deprivation, which are rampant in poorly vascularized areas of tumors *in vivo*. They also can recover from damage induced by heat. Regardless of the type of damage, all DR cells exhibit increased aerobic glycolysis, enhanced ATP production, rapid *in vitro* and *in vivo* proliferation, and resistance to damage. In support of such *in vitro* induced damage recovery, DR cells that are isolated from *in vivo* generated tumors also exhibit increased aerobic glycolysis and a high proliferation rate. These results are consistent with those reported by Heller and Raaphorst who showed that glioblastoma cells that recover from radiation-induced damage display increased proliferation rate and increased glucose consumption [15]. Thus, regardless of cause of damage, all DR cells display increased glycolytic activity. This shows that instead of deriving energy from oxidative phosphorylation as it occurs in somatic cells, the consequence of damage recovery is a decrease in cellular oxidative capacity and heavy reliance on aerobic glycolysis.

In a recent study, it was shown that tumor cells that survive acidotic conditions demonstrate elevated markers of autophagy and not only become damage tolerant but they become dependent on low pH for prolonged survival [18]. Our data show that the development of such features might all be related to damage recovery. Tumor cells that recover from hypoxia, glucose deprivation or acidosis become tolerant to the initial damaging condition and may also develop cross tolerance to other types of damage.

A decline in mitochondrial numbers and changes in mitochondrial DNA copy number have been detected in numerous advanced cancers that show a high degree of malignancy [19–21]. We find that the cells that recover from damage induced by hypoxia, glucose deprivation or acidosis show reduced mtDNA, as well as tolerance to damage and a high proliferation rate providing a link between damage recovery and malignant behavior. This is seen in patients who are treated with radiation yet their tumors show an accelerated course of cancer progression [22]. Since hypoxia, glucose deprivation and extracellular acidosis all occur in tumors, cycles of damage and recovery by any of these damaging conditions might underlie tumor progression and development of more malignant phenotype in cancers [22].

Our findings link bioenergetic metabolic remodeling in cells recovered from damage to the reorganization of mitochondrial network. In damage recovered cancer cells, in parallel with loss of cristae, the number of mitochondria decreases while their size increases. Hypoxia has been shown to lead to reduction in number of cristae in neuronal cells. More importantly, in neurons that were treated with camptothecin, acidosis-induced mitochondrial restructuring occurs and these cells become resistant to stress [23]. It has been previously shown that in cancer cells, heightened aerobic glycolysis is indispensable to the increase in biomass and rapid cell division [2]. Thus, it appears that the mitochondrial restructuring results directly from the damaging condition, drives reliance on aerobic glycolysis for damage repair and promotes rapid cell proliferation.

Taken together, our data suggest that even a small subset of tumor cells that recover from damage can give rise to a new generation of damage resistant cells that contribute to the expansion of cancer cell pool and facilitate their adaptation to a new environment.

Acknowledgment

The authors declare no conflict of interest.

References

[1] S.K. Parks, J. Chiche, J. Pouysségur, Disrupting proton dynamics and energy metabolism for cancer therapy, Nat. Rev. Cancer 13 (2013) 611–623.
[2] M.G. Vander Heiden, L.C. Cantley, C.B. Thompson, Understanding the Warburg effect: the metabolic requirements of cell proliferation, Science 324 (2009) 1029–1033.
[3] S.P. Mathupala, Y.H. Ko, P.L. Pedersen, The pivotal roles of mitochondria in cancer: Warburg and beyond and encouraging prospects for effective therapies, Biochim. Biophys. Acta 1797 (2010) 1225–1230.
[4] S.K. Parks, J. Chiche, J. Pouysségur, PH control mechanisms of tumor survival and growth, J. Cell. Physiol. 226 (2011) 299–308.
[5] H.R. Christofk, M.G. Vander Heiden, M.H. Harris, A. Ramanathan, R.E. Gerszten, R. Wei, M.D. Fleming, S.L. Schreiber, L.C. Cantley, The M2 splice isoform of pyruvate kinase is important for cancer metabolism and tumour growth, Nature 452 (2008) 230–233.
[6] S. Gottschalk, N. Anderson, C. Hainz, S.G. Eckhardt, N.J. Serkova, Imatinib (STI571)-mediated changes in glucose metabolism in human leukemia BCR-ABL-positive cells, Clin. Cancer Res. 19 (2004) 6661–6668.
[7] J.S. Flier, M.M. Mueckler, P. Usher, H.F. Lodish, Elevated levels of glucose transport and transporter messenger RNA are induced by ras or src oncogenes, Science 235 (1987) 1492–1495.
[8] R.L. Elstrom, D.E. Bauer, M. Buzzai, R. Karnauskas, M.H. Harris, D.R. Plas, H. Zhuang, R.M. Cinalli, A. Alavi, C.M. Rudin, C.B. Thompson, Akt stimulates aerobic glycolysis in cancer cells, Cancer Res. 64 (2004) 3892–3899.
[9] R.A. Gatenby, R.J. Gillies, Why do cancers have high aerobic glycolysis?, Nat Rev. Cancer 4 (2004) 891–899.
[10] H. Pelicano, D.S. Martin, R.H. Xu, P. Huang, Glycolysis inhibition for anticancer treatment, Oncogene 25 (2006) 4633–4646.
[11] J. Zheng, Energy metabolism of cancer: glycolysis versus oxidative phosphorylation, Oncol. Lett. 4 (2012) 1151–1157.
[12] M. Wu, A. Neilson, A.L. Swift, R. Moran, J. Tamagnine, D. Parslow, S. Armistead, K. Lemire, J. Orrell, J. Teich, S. Chomicz, D.A. Ferrick, Multiparameter metabolic analysis reveals a close link between attenuated mitochondrial bioenergetic function and enhanced glycolysis dependency in human tumor cells, Am. J. Physiol. Cell Physiol. 292 (2007) C125–C136.
[13] Min Fang, Zhirong Shen, Song Huang, Liping Zhao, She Chen, Tak W. Mak, Xiaodong Wang, The ER UDPase ENTPD5 promotes protein N-glycosylation, the Warburg effect, and proliferation in the PTEN pathway, Cell 143 (5) (2010) 711–724.
[14] R.A. Phillips, I.J. Tolmach, Repair of potentially lethal damage in x-irradiated HeLa cells, Radiat. Res. 29 (1966) 413–431.
[15] D.P. Heller, G.P. Raaphorst, Inhibition of potentially lethal damage recovery by altered pH, glucose utilization and proliferation in plateau growth phase human glioma cells, Int. J. Radiat. Biol. 66 (1994) 41–47.
[16] M.E. Varnes, L.A. Dethlefsen, J.E. Biaglow, The effect of pH on potentially lethal damage recovery in A549 cells, Radiat. Res. 108 (1986) 80–90.
[17] D.P. Heller, M.M. Feeley, G.P. Raaphorst, Changes in survival and potentially lethal damage recovery following periods of high and low metabolic activity in human glioma cells, Oncol. Res. 5 (1993) 475–482.
[18] J.W. Wojtkowiak, J.M. Rothberg, V. Kumar, K.J. Schramm, E. Haller, J.B. Proemsey, M.C. Lloyd, B.F. Sloane, R.J. Gillies, Chronic autophagy is a cellular adaptation to tumor acidic pH microenvironment, Cancer Res. 72 (2012) 3938–3947.
[19] Y. Onishi, T. Ueha, T. Kawamoto, H. Hara, M. Toda, R. Harada, M. Minoda, M. Kurosaka, T. Akisue, Regulation of mitochondrial proliferation by PGC-1α induces cellular apoptosis in musculoskeletal malignancies, Sci. Rep. 4 (2014) 3916–3923.
[20] S. Yamada, S. Nomoto, T. Fujii, T. Kaneko, S. Takeda, S. Inoue, N. Kanazumi, A. Nakao, Correlation between copy number of mitochondrial DNA and clinicopathologic parameters of hepatocellular carcinoma, Eur. J. Surg. Oncol. 32 (2006) 303–307.
[21] O. Delgado, K.G. Batten, J.A. Richardson, X.J. Xie, A.F. Gazdar, A.A. Kaisani, L. Girard, C. Behrens, M. Suraokar, G. Fasciani, W.E. Wright, M.D. Story, I.I. Wistubal, J.D. Minna, J.W. Shay, Radiation-enhanced lung cancer progression in a transgenic mouse model of lung cancer is predictive of outcomes in human lung and breast cancer, Clin. Cancer Res. 20 (2014) 1610–1622.
[22] M. Yu, Y. Zhou, Y. Shi, L. Ning, Y. Yang, X. Wei, N. Zhang, X. Hao, R. Niu, Reduced mitochondrial DNA copy number is correlated with tumor progression and prognosis in Chinese breast cancer patients, IUBMB Life 59 (2007) 450–457.
[23] M. Khacho, M. Tarabay, D. Patten, P. Khacho, J.G. MacLaurin, J. Guadagno, R. Bergeron, S.P. Cregan, M.E. Harper, D.S. Park, R.S. Slack, Acidosis overrides oxygen deprivation to maintain mitochondrial function and cell survival, Nat. Commun. 5 (2014) 3550–3564.